INVESTIGATION ON PROCESS INDUCED NANO SCALE SHAPE DEVIATIONS OF DUV TUNGSTEN WIRE GRID POLARIZER

Thomas Siefke, Daniel Voigt, Oliver Puffky and Ernst-Bernhard Kley

Institute of Applied Physics, Albert-Einstein-Straße 15, 07745 Jena, Germany
E-mail: Thomas.Siefke@uni-jena.de

ABSTRACT

Wire grid polarizers are nano optical devices offering the possibility to achieve linear polarized light. Especially in the DUV spectral range these elements overcome conventional solutions. In the past such elements were successful fabricated by us and utilized in several applications. However, the experimentally achieved optical performance is far below expected. This can be explained by deviations of the refractive index as well as the geometry. Within this contribution both are examined by numerical methods. For this purpose a refined geometry model is presented and its plausibility is shown. Thereby the agreement between simulation and measurement is significantly emended. Following, the model is used to assess the influence of particular shape deviations according to their severity. Thereby the most promising approaches for future process improvements are revealed.

Index Terms – Wire grid polarizer, DUV, shape deviations, rigorous coupled wave analysis

1. INTRODUCTION

Polarization is an essential feature of electromagnetic radiation and therefore relevant in many areas of optical science and technology. On the one hand, several analytical methods, such as ellipsometry [1] are basing on the setting and measurement of a particular polarization state or additional information can be obtained as in spectroscopy or microscopy. On the other hand, nano patterning methods such as optical lithography [2, 3] can be improved by setting a specific polarization state. The current development in these fields tends to shorter wavelength in the UV spectral range. Especially from 230 nm to 350 nm tungsten wire grid polarizer overcome the possibility of conventional devices in terms of large element area, small overall height and a broad acceptance angle. Therefore the interest in such devices grew rapidly in recent years.

Wire grid polarizer consist of parallel metal ridges with a period below the wavelength of the incident light at an aspect ratio of typically 6 to 10. The transmittance of such nano optical devices strongly differs for the polarization direction of the incident light, relative to the ridges. To achieve linear polarized light, in a broad wavelength range, the transmittance of the parallel component (T_{TE}) has to be much smaller than the transmittance of the orthogonal component (T_{TM}). The optical performance is commonly characterized by the transmittance of TM polarized light and the extinction ratio $ER = T_{TM}/T_{TE}$. Although well performing wire grid polarizers were fabricated, the performance of these devices is typically substantially lower than predicted by numerical simulations, utilizing a binary grating structure and refractive index values from literature [1]. Especially the extinction ratio differs by a factor of 40 (Figure 1). This prevents a targeted improvement of the fabrication method and complicates a reliable design process. Thus the aim of this work is to explain these differences, provide an improved model for numerical simulations and derive practical approaches for the improvement of the fabrication process.

There are two possible origins for the deviations. These are, one the one hand the material properties of the ridges, on the other hand the geometry of the grating structure. Firstly, the impact of the refractive index is estimated by comparing the simulated performance for two different material parameters. Secondly, a more detailed geometry model is provided, its plausibility is examined and the influences of the particular features to the optical performances are assessed. It has been shown for other nano optical devices as plasmonic nano rings [2, 3] or photonic crystals [4] that even minor geometrical differences have a large impact on the optical behavior. Within this contribution both influences are examined by means of rigorous coupled wave analysis (RCWA) [5].
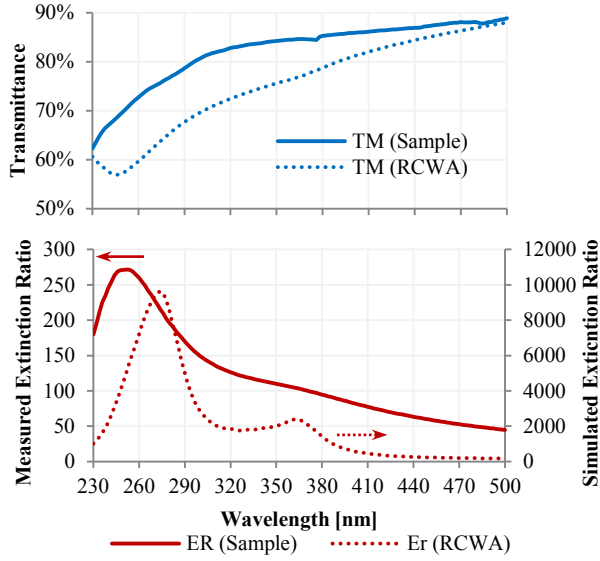
Figure 1: Comparison between simulated (RCWA) and measured optical properties. Please note: the measured extinction ratio is magnified by a factor of 40.

2. DESIGN OF THE IDEAL GEOMETRY

Although highly dependent on the particular application an extinction ratio of about 100 and a transmittance of about 50% is commonly required for optical devices. In the spectral range from 230 nm to 350 nm tungsten was shown to be appropriate [6]. Initially the wire grid polarizer is described as binary grating (Figure 2) with a period p, a ridge height h and a ridge width d. To achieve a first design, RCWA simulations were performed based on the intended optical requirements and consideration of fabrication constrains. Thereby a period of 100 nm, a ridge height of 150 nm and a ridge width of 23 nm is found. This geometry will be referred to as ideal geometry within this contribution.
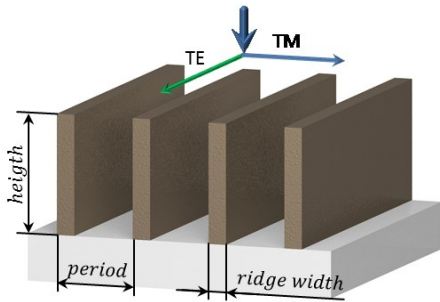

Figure 2: Schematic of a wire grid polarizer. Design parameter height, period and ridge width as well as TE and TM direction are marked.
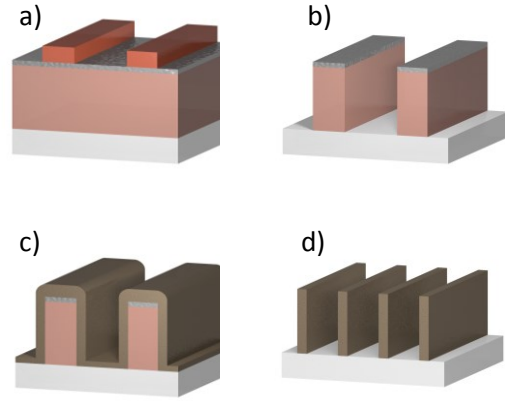
3. PROCESS

Figure 3: Fabrication process of tungsten wire grid polarizer; a) initial layer stack b) etched template structure c) tungsten deposited on template d) final wire grid polarizer

For the fabrication of tungsten wire grid polarizer a self-aligned double patterning (SADP) [7] process is utilized [8, 6, 9, 10]. Thereby the necessary period and height aspect ratios are achieved. For that purpose an initial layer stack of polymer, chromium and an electron beam photoresist is prepared by spin coating and ion beam deposition (IBD). Afterwards the initial template grating structure is defined by electron beam lithography (Figure 3, a). For the electron beam lithography a SB350OS from Vistec is utilized. This tool includes a character aperture in the beam line. Thereby the writing speed is enhanced by several orders of magnitude compared to tools using a Gauß shaped electron beam [11]. This allows the appropriate patterning of a grating with a period of 200 nm and a size of 100 cm² in about 8 h. Subsequently the chromium and the polymer are etched by means of ion beam etching (IBE) and reactive ion beam etching (RIBE) respectively (Figure 3, b). In a next step tungsten is deposited by IBD under a shallow angle (Figure 3, c). The following step is the removal of the material on the horizontal surfaces by IBE. Finally the initial template grating is removed by means of RIBE (Figure 3, d).

2

4. REFINED GEOMETRY MODEL
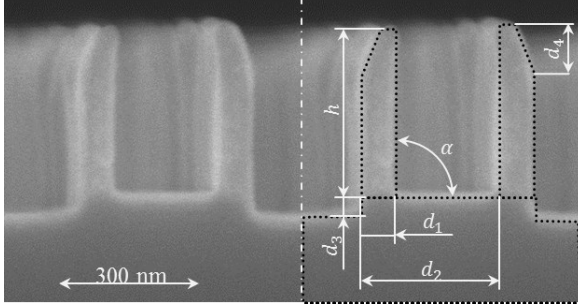
Determination of the refined geometry model

Figure 4: Cross sectional SEM image of a tungsten wire grid polarizer. The geometrical model is inserted and the according parameters are marked.

In order to determine the deviation between predicted and measured optical performance a cross sectional SEM image is considered (Figure 4). Compared to the ideal binary grating structure (Figure 2) various differences are conspicuous. To include these discrepancies in the RCWA simulations a more complex geometrical model is applied (see dotted line Figure 4). From this model the set of examined geometrical parameters in expanded to the ridge height h, ridge width d_1, displacement d_2 , depth of the trench d_3, height of the chamfer d_4 and the tilt of the ridges α.

The height h of the ridges is mainly defined by the initial thickness of the polymer although further steps reduce it as well. During the double patterning process the period of the template grating is halved to the period of the wire grid polarizer (see Figure 2). While this is considered as perfect due to the electron beam tool [11], the line width of the template grating may change. Therefore the displacement d_2 between two adjacent ridges may differ from the halve template grating period. The thickness of the ridges d_1 is at the one hand defined by the deposition process and at the other hand by secondary sputter deposition of the material from the bottom of the grating structure. During this etching a trench with a depth d_3 is generated. Additionally the angle dependence of IBE lends to a preferential etch on edges. Therefore the ridges are chamfered to a certain length d_4. It is assumed that the chamfer starts at the halve ridge width to account for the less affected edge, were the template was located. Although not visible in Figure 4, a sloped sidewall of the template grating causes the ridges to bend inwards. This is described by the tilt of the ridges α. Other distortions are disregarded.

In order to evaluate the dependency on each individual parameter, the optical performance is simulated by means of RCWA, varying the particular value and keeping the others fixed at the ideal geometry. The outcome is, at the one hand, additionally wavelength dependent, on the other hand non-linear. To allow for a comparison of the influence of the individual parameter a figure of merit is introduced. Therefore the slope of a linearization in a small region around the point of the ideal geometry is utilized. The width of this region is determined from expected process deviations. This allows the assessing of the severity of the specific influence to the optical performance.

Assessment of the refined geometry model

For the assessment of the refined geometry model, possible geometry deviations are estimated and the simulation is compared to a measurement. A ridge height of 130 nm, a ridge width of 20 nm, a displacement of 94 nm, a chamfer height of 30 nm, a tilt of 3° and a trench depth of 20 nm is assumed. Regarding the simulated transmittance --a feature at 350 nm is noticeable. The same feature arises at the measured values but red shifted by about 20 nm. At a wavelength of 298 nm a sudden change of the slope occurs for both simulated and measured values, Noteworthy, this feature is not present in the results of the simple model (Figure 1). The maximum of the measured extinction ratio is shifted by about 20nm to shorter wavelength. The features above 290 nm of the measured curve is obscured but reproduced by the simulation. Furthermore the magnitude of the transmittance as well as the extinction ratio is very similar between simulation and measurement. Therefore, it is concluded that the model is applicable to the asses the individual influences.
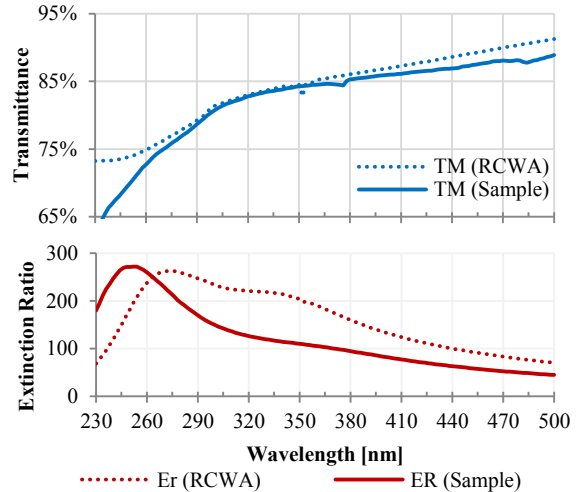

Figure 5: Comparison between simulated and measured optical performance. For the simulation the refined model is utilized.

3

5. INFLUENCE OF DEVIATIONS TO THE OPTICAL PERFORMANCE

Refractive index deviations

The refractive index of the deposited material is measured at a tungsten layer on a silicon substrate with a thickness of 80 nm. For this purpose a Sentech SE 850 variable angle spectroscopic ellipsometer (VASE) is utilized. Compared to bulk material data [1] (Figure 6) the measured thin film refractive index is smaller, and the absorption coefficient is larger, both showing less pronounced features. To assess the influence on the optical performance both data are used to simulate the ideal polarizer geometry (*Figure 7*). Particularly conspicuous is the large peak at 300 nm of the extinction ratio. At this position the extinction ratios are differing by about one order of magnitude while the complex refractive index merely differs by about 20 %.
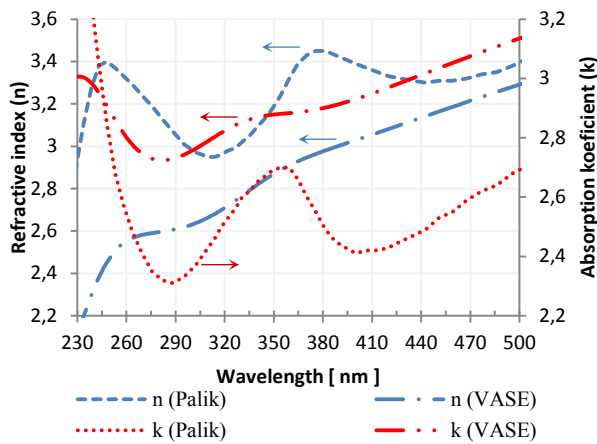

Figure 6: Comparison between refractive index and absorption coefficient from literature [1] and value measured by variable angle spectroscopic elipsometry.
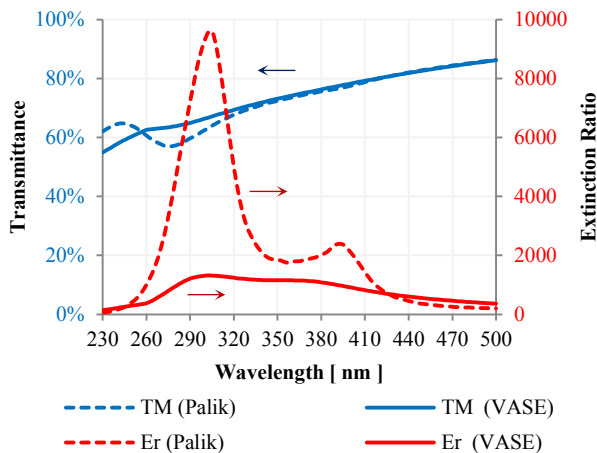

Figure 7: Simulated optical performance for bulk material refractive index of tungsten from literature [1] compared to simulations with e measured thin film refractive index (Figure 6).

Shape deviations

Ridge height

An increase of the ridge height causes a decrease of the transmittance almost independent from wavelength (Figure 8). The transmittance of TM polarized light is linearly changed (Figure 9) the slope is $0.3\,\%/nm$. The extinction ratio strongly increases by an increase of the ridge height due to an exponential correlation (Figure 9). This change is less pronounced for wavelength below 260 nm and above 470 nm the shape of the curve is not altered (Figure 8). The influence of small deviations is $5\,\%/nm$.
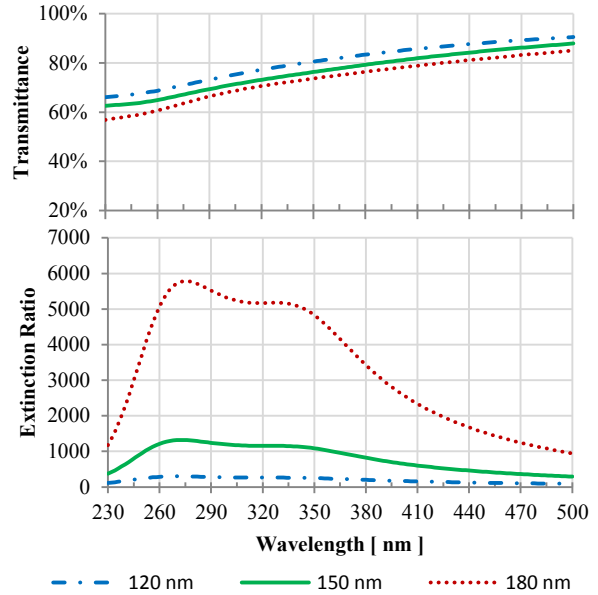

Figure 8: Simulated optical performance at ridge heights of 120 nm, 150 nm and 180 nm. The wavelength is varied from 230 nm to 500 nm. The intended ridge height is 150 nm.
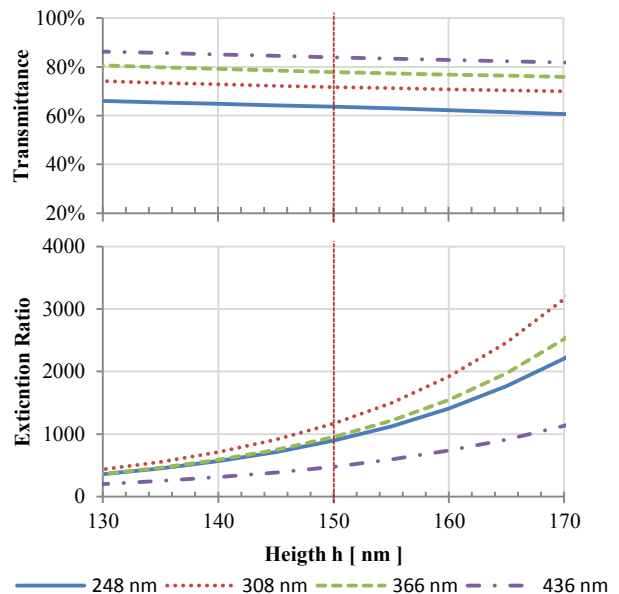

Figure 9: Simulated optical performance at different wavelengths for a ridge height from 130 nm to 170 nm. The intended ridge height is 150 nm.

Ridge width

An increase of the ridge width linearly decreases the transmittance (Figure 11). In comparison to the ridge height this change is stronger wavelengths dependent. The influence is more pronounce at shorter wavelength (Figure 10) the slope is $-3\,\%/nm$. The influence to the extinction ratio is exponential (Figure 11) the figure of merit determined as $21\,\%/nm$. Again the impact is more pronounced between 260 nm and 460 nm.
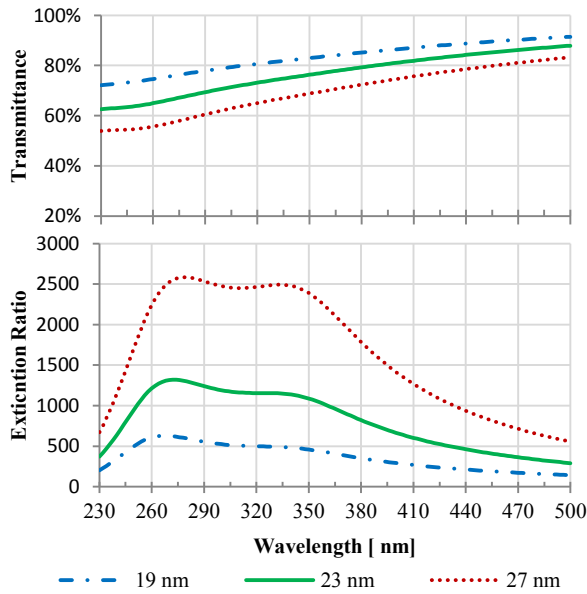

Figure 10: Simulated optical performance at ridge width of 19 nm, 23 nm and 27 nm. The wavelength is varied from 230 nm to 500 nm. The intended ridge width is 23 nm.
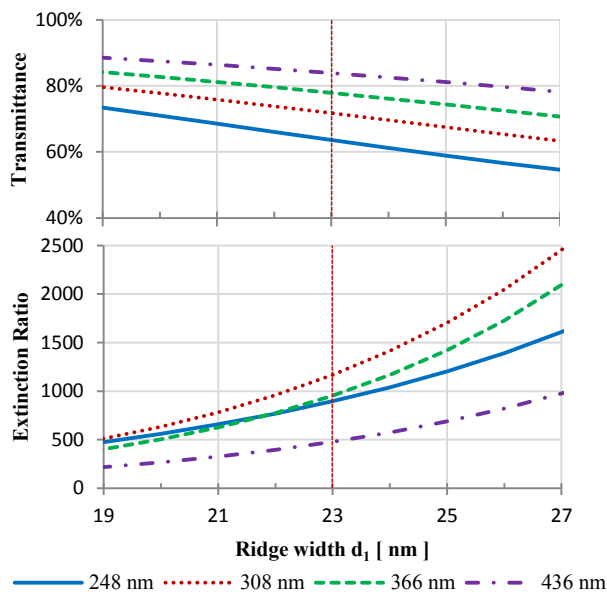

Figure 11: Simulated optical performance at different wavelengths for a ridge width from 19 nm to 27 nm. The ideal ridge width is 23 nm.

Displacement

Inherent to the SADP process is that non-suitable line width of the template grating causes asymmetric distances between adjacent ridges, thus introducing a periodic disturbance at twice the grating period, in this case 200 nm. Therefore diffraction occurs for wavelength below 298 nm. While the influence to the transmittance is negligible (Figure 12 & Figure 13), the extinction ratio is strongly influenced below this wavelength. In the first place additional features are introduced e.g. the quick drop around 298 nm of the extinction ratio at a displacement of 112 nm (Figure 12). Furthermore the extinction ratio is substantially lowered below this point. The figure of merit determined as $-5\%/nm$.
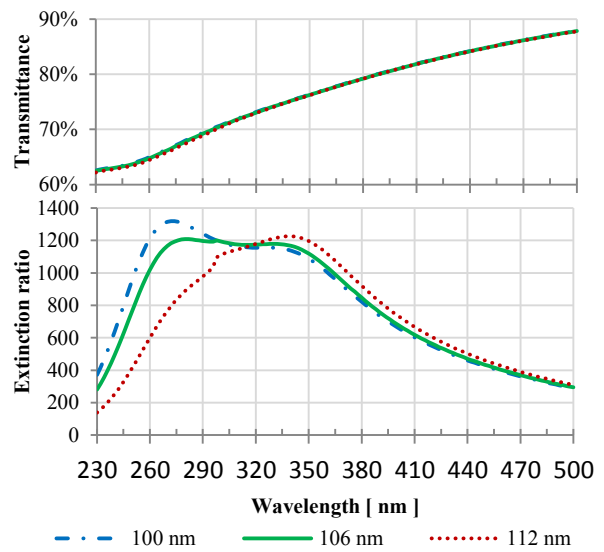

Figure 12: Simulated optical performance at displacement of 100 nm, 106 nm and 112 nm. The wavelength is varied from 230 nm to 500 nm. The intended displacement is 100 nm.
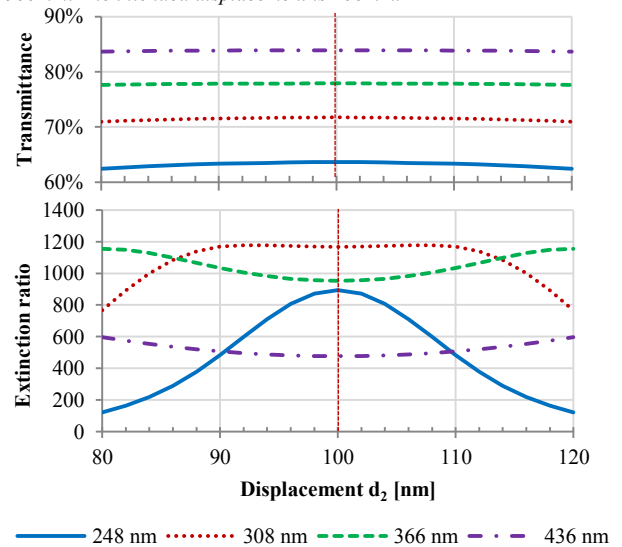

Figure 13: Simulated optical performance at different wavelengths for a displacement from 80 nm to 120 nm. The ideal value is 100 nm.

Chamfer

The chamfer at the tips of the ridges is in a first place equivalent to a minor, local reduction of the ridge width. However an additional asymmetry at the period of the template grating arises, causing diffraction below 298 nm. Regardless no additional wavelength dependent features are noticeable (Figure 14). An increase of the chamfer height slightly increases the transmittance by $0.2\,\%/nm$ while the extinction ratio decreases by about $-0.7\,\%/nm$ (Figure 15).

Trench depth

The depth of the trench in the substrate can be interpreted as the height of an additional fused silica grating below the polarizer with doubled period. Thereby diffraction is caused and the interaction of electromagnetic fields with the substrate is altered. However the influence to the transmittance of $-0.02\,\%/nm$ is small (Figure 17) but slightly more pronounced at wavelength below 300 nm (Figure 16). Although more pronounced between 260 nm and 460 nm wavelength (Figure 16), the effect on the extinction ratio is linear with a slope of $-0.7\,\%/nm$ (Figure 17).
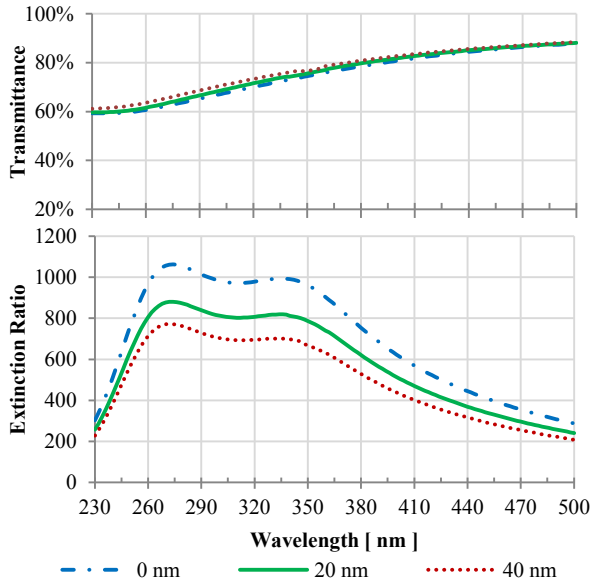

Figure 14: Simulated optical performance at chamfer height of 0 nm, 20 nm and 40 nm. The wavelength is varied from 230 nm to 500 nm. A chamfer is not intentionally created.
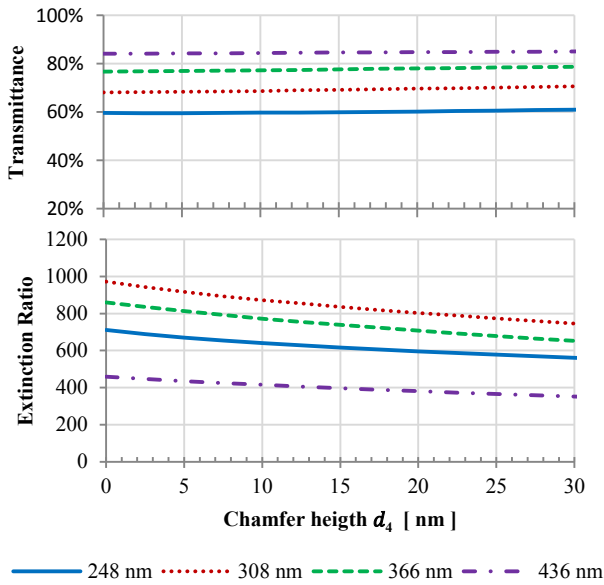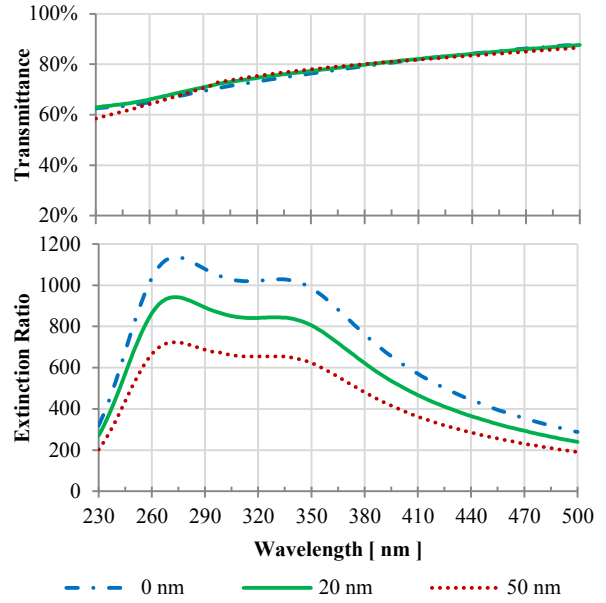

Figure 16: Simulated optical performance at trench depth of 0 nm, 20 nm and 50 nm. The wavelength is varied from 230 nm to 500 nm. A trench is not intentionally created

Figure 15: Simulated optical performance at different wavelength for a chamfer height from 0 nm to 30 nm. Ideally no chamfer arises.
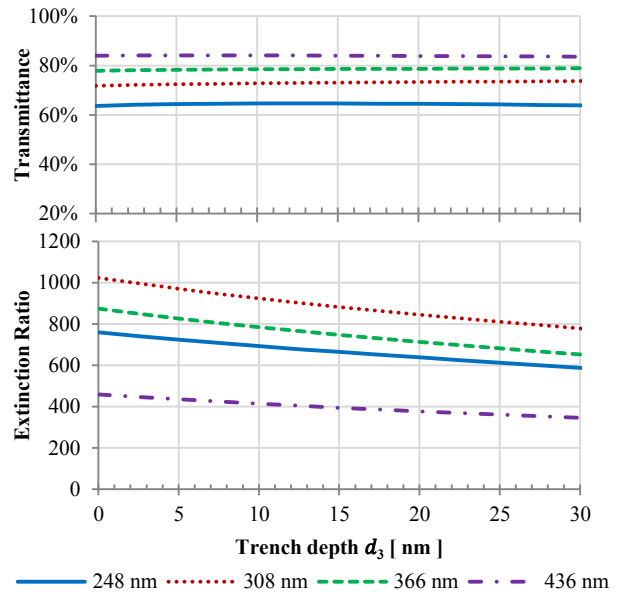

Figure 17: Simulated optical performance at different wavelength for a trench depth from 0 nm to 30 nm. Ideally no trench arises.

Tilt

A tilt of the ridges again introduces an asymmetry, causing diffraction and associated features in the extinction ratio at 298 nm wavelength (Figure 18). Additionally features at 350 nm occur at both extinction ratio and transmittance (Figure 18). It is believed that resonance effects are responsible for this. Excluding these features, the influence on the transmittance can be regarded as linear in the considered range and is about −0.4 %/° (Figure 19). The maximum of extinction ratio is basically red shifted by an increased tilt. Therefor the influence is more pronounced for wavelength below 350 nm while larger wavelengths are less affected (Figure 18). As figure of merit −11 %/° is determined.
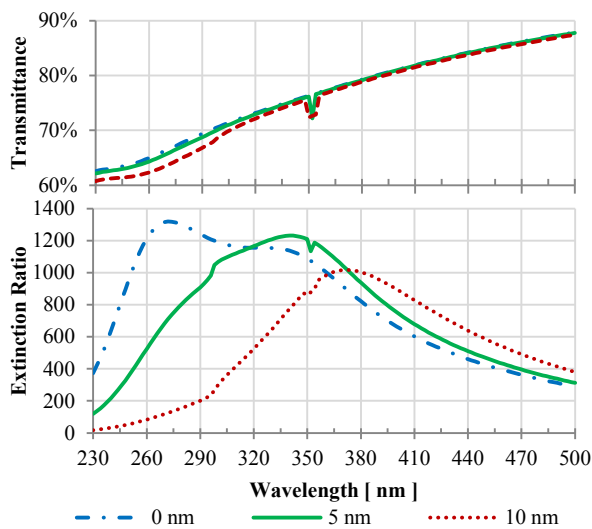

Figure 18: Simulated wavelength dependent transmittance and extinction ratio for variation of the tilt of 0°, 5°and 10°.
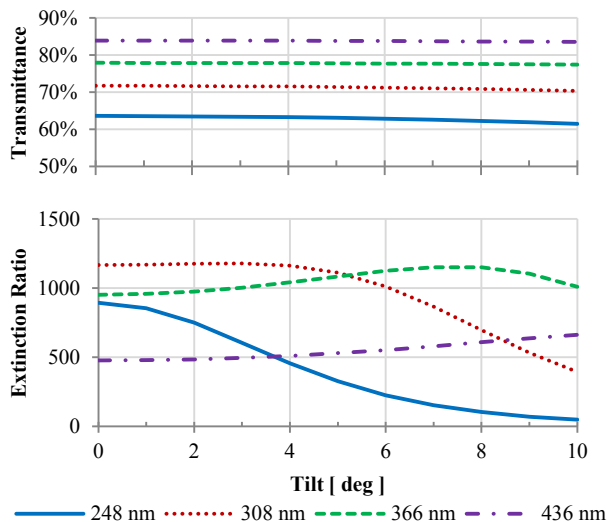

Figure 19: Simulated optical performance at different wavelength for a tilt from 0° to 10°.

6. DISCUSSION

In the first instance the obtained results show that the influence of the refractive index is very large. Slight changes of several percent result in a change of the extinction ratio by about one order of magnitude. This is especially problematic considering that the actual refractive index of the ridges is barely accessible and may be additionally altered by film thickness dependence, surface oxidation, lattice damage due to energetic ions impinging during etching or by intermixing with template or substrate material. However by applying more reasonable material properties the agreement between simulation results and measurements are significantly improved. For a further refinement, shape deviations are taken into account by a more sophisticated geometry model. To verify the plausibility of this model a simulation is done using this geometry model and parameters estimated from fabrication experiences. Although these estimations are roughly, the agreement to the measurement results is appropriate, regarding the achieved magnitude. Furthermore, features in the transmittance which are assumed to be caused by resonance effects at 350 nm are reproduced, but slightly shifted. An additional feature at 298 nm caused by diffraction is apparent at both measurement and improved simulation, but not at simulations done with the simple geometry model (Figure 7). The general shape of the extinction ratio is reproduced by simulations. However the maximum is slightly shifted to shorter wavelength. The shifted and obscured features of the transmittance as well as extinction ratio can be caused by a deviation of the actual complex refractive index of the ridges as previously discussed.

In conclusion the refined model is adequate to explain the measured behavior of the optical performance. Deviations between both are conceived and addressed mainly to the unknown actual material properties.

By applying the advanced model and varying the individual parameters it is shown that, shape deviations, have a larger influence on the extinction ratio, than on the transmittance of TM polarized light. Furthermore by assessing the severity of the influence of the individual deviations using a figure of merit, it is found that the width and the tilt of the ridges show the most severe impact. The smaller influence of the displacement and height are almost equal in size but contrary. The impairment caused by the chamfer and the trench depth is the smallest. However, regarding the trench depth it is currently not clarified if material removed from the trenches deposit on and intermixes with the ridges. Thereby a severe altering of material properties can be caused which in turn causes an even more severe impairment on the optical properties.

7. SUMMARY

Within this work the deviation between expected and achieved optical performance of tungsten wire grid polarizer is revealed. In a first place complex refractive index deviations have an influence of about one order of magnitude, which is the most significant. Additionally the influence of shape deviations is examined. For this purpose a refined geometry model is identified and its plausibility is confirmed. By means of this model the influence of particular shape deviations are assessed regarding their severity. In the first place it is found that the extinction ratio is more vulnerable to deviations than the transmittance. The most severe impairment is caused by deviations of the width and tilt of the ridges. A decrease of the ridge width by one nanometer causes 20 % reduction of the extinction ratio and tilt of the ridges by 1° causes a decrease of the extinction ratio by 10%. Therefore future improvement of tungsten wire gird will focus on material properties, ridge width and tilt.

8. ACKNOWLEDGMENTS

9. REFERENCES

[1] H. G. Tompkins and E. A. Irene, Handbook of ellipsometry, Norwich, NY: Springer, 2005.

[2] D. Flagello, B. Geh, S. Hansen and M. Totzeck, "Polarization effects associated with hyper-numerical-aperture (>1) lithography," *J. Micro/Nanolith. MEMS MOEMS,* no. doi:10.1117/1.2039081, 2005.

[3] A. M. Zibold, W. Harnisch, T. Scherübl, N. Rosenkranz and J. Greif, "Using the aerial image measurement technique to speed up mask development for 193nm immersion and polarization lithography," *Proceedings of SPIE,* 2004.

[4] E. D. Palik, "Handbook of optical Constants of Solids," *Academic Press,* vol. 3, no. 1998.

[5] D. Lehr, K. Dietrich, C. Helgert, T. Käsebier, H.-J. Fuchs, A. Tünnermann and E.-B. Kley, "Plasmonic properties of aluminum nanorings gernerated by double patterning," *Opt. Lett,* vol. 37, no. 2, pp. 157-159, 2012.

[6] N. Large, J. Aizpurua, V. K. Lin, S. LangTeo, R. Marty, S. Tripathy and A. Mlayah, "Plasmonic properties of gold ring-disk nano-resonators: fine shape details matter," *Opt. Exp.,* vol. 19, no. 6, pp. 5587-5595, 2011.

[7] R. C. Rumpf, Design and optimization of nano-optical elements by coupling fabrication to optical behavior, Orlando, 2006.

[8] M. Moharam and T. Gaylord, "Rigorous coupled-wave analysis of metallic surface-relief gratings," *J. Opt. Soc. Am. A,* vol. 3, no. 11, pp. 1780-1787, 1986.

[9] T. Weber, T. Käsebier, M. Helgert, E.-B. Kley and A. Tünnermann, "Tungsten wire grid polarizer for applications in the DUV spectral range," *Appl. Opt.,* vol. 51, no. 16, pp. 3224-3227, 2012.

[10] P. Zimmerman, "Double patterning lithography: double the trouble or double the fun?," *SPIE Newsroom,* 2009.

[11] T. Weber, Mikrooptischer Polarisator für den UV-Spektralbereich, Jena, 2008.

[12] T. Weber, T. Käsebier, E.-B. Kley and A. Tünnermann, "Broadband iridium wire grid polarizer for UV applications," *Opt. Lett.,* vol. 36, no. 4, pp. 445-447 , 2011.

[13] T. Weber, T. Käsebier, A. Szeghalmi, M. Knez, E.-B. Kley and A. Tünnermann, "High aspect ratio deep UV wire grid polarizer fabricated by double patterning," *Microelectronic Engineering,* vol. 98, no. 2, p. 433–435, 2012.

[14] E.-B. Kley, H. Schmidt, U. Zeitner, M. Banasch and B. Schnabel, "Enhanced E-beam pattern writing for nano-optics based on character projection," *Proc. of SPIE,* no. 8352, 2012.